# Rotary Wing UAV System Identification for flight control design

**Filippo Zanetti [1], Barbara Teodorani [2], Gian Marco Saggiani [3], Roberto Pretolani [4]**

[1] II School of Engineering - University of Bologna
Via Fontanelle 40, 47100 Forlì, Italy
e-mail: filippo.zanetti@unibo.it

[2] II School of Engineering - University of Bologna
Via Fontanelle 40, 47100 Forlì, Italy
e-mail: barbara.teodorani@ingfo.unibo.it

[3] II School of Engineering - University of Bologna
Via Fontanelle 40, 47100 Forlì, Italy
e-mail: gianmarco.saggiani@unibo.it

[4] II School of Engineering - University of Bologna
Via Fontanelle 40, 47100 Forlì, Italy
e-mail: pretolani@ingfo.unibo.it

**Key words**: Rotary wing UAV, identification, model, control, state space

**Abstract.** This paper presents the results, achieved at the Aerospace Engineering Department Laboratories of the University of Bologna, concerning the development of a simple identification procedure, in a Matlab-Simulink environment, in order to obtain a representative dynamic model of a small rotorcraft UAV near hovering flight conditions. Procedure starts with open-loop identification test flights without any cross-effect accounted, cross-effects are then introduced in the simulated model and, at the end, parameters refinement is performed using a closed loop identification technique. For each step, training data are shown and the adopted cost function to be minimized is described. Moreover cross validation is performed and indexes of relative goodness of fit are computed to assess the new model.

Symbols legend:

| | |
|---|---|
| $a,b$ | longitudinal and lateral rotor flapping |
| $\phi,\theta$ | longitudinal and lateral attitude angles |
| $p,q$ | roll, pitch rates in helicopter reference frame |
| $u,v,w$ | longitudinal, lateral and vertical speed in body reference frame |
| $\delta lon, \delta lat, \delta coll$ | cyclic longitudinal, lateral, collective control inputs |
| g | (9.81 m/s$^2$) acceleration of gravity |
| $\tau_e$ | main rotor time constant |
| $\omega_{np}$ $\omega_{nq}$ | lateral and longitudinal fuselage-rotor-bar natural frequencies |
| $A_{lon}$, $B_{lat,}$, $X_u$. $Y_v$, $X_a$, $Y_b$, $L_b$, $M_a$, $Z_{coll}$, $Z_w$ | On-axis derivatives |
| $M_u$, $M_v$, $L_u$, $L_v$ | Speed derivatives |
| $A_{lat}$, $B_{lon}$, $M_b$, $L_a$, $M_{coll}$ | Off-axis derivatives |

## 1. INTRODUCTION

It is well known that Unmanned Air Vehicles (UAVs) may represent a promising and cost-effective alternative to manned aircraft for a large number of civil applications. Compared to traditional air vehicles, UAVs may, in fact, offer significant advantages in terms of human safety (especially in dull, dirty and dangerous missions), operational cost reduction and work rate efficiency. In particular Rotorcraft UAV (RUAV) systems, due to their versatile flight modes, maneuverability and vertical take-off and landing capabilities, represent even a more promising solution than fixed wing UAVs.

In the last years UNIBO has developed an unmanned small scale helicopter that is now capable of autonomous flight and that can be used inside the Universities as a platform for researches in control and navigation laws, meanwhile it could be proposed as a technological prototype for industries interested in UAV development and manufacturing. In order to take advantage of existing and cost effective technology, UNIBO has used Commercial Of The Shelf (COTS) sensors and electronics for its RUAV avionics package.

The analysis and design of a good flight control system requires the knowledge of an accurate model of vehicle dynamics [1]: such model can be obtained using the known System identification techniques used for bigger machines, with some simplifications.

Aim of this paper is to present a simple System Identification Procedure for Control Design. In particular the identified system shall be used, in the future, to compare performances of a traditional PID controller versus a feed-forward control algorithm based on dynamic model inversion (both for longitudinal and lateral dynamics). The proposed time-domain identification procedure is entirely developed in Matlab-Simulink environment, and requires no other external software applications.

This paper is made of four parts; in the first a brief description of UNIBO RUAV is given. Second part is about Open-Loop (OL) identification without cross-effects, the third introduces cross-effects while in last part parameters refinement is performed using a Closed Loop (CL) identification technique. Results will demonstrate how the proposed Identification procedure provides a model showing a good agreement especially in closed loop validation accounting also for cross-axis effects.

## 2. UNIBO ROTORCRAFT UAV

The Bologna University Rotary Wing UAV, shown in the Figure 1, is built around a modified Hirobo Eagle II 60 hobby helicopter with a more powerful engine, longer fiberglass blades (main and tail rotor) and longer tail boom. The new main rotor is a 2 blades see-saw type with Bell-Hiller stabilizer with a diameter of 1.84 m and the total mass is about 11.2 kg. A National Instruments CompactRIO system has been selected as flight computer and performs both the task of Autopilot and FMS. For flight data measurement a Crossbow NAV420 GPS-aided Attitude Heading Reference System (AHRS) and ultrasonic sensors have been installed which provide accurate signals in velocity, flight altitude and helicopter attitude. In such a way, the University of Bologna, through a rapid prototyping approach, has been the first Italian University achieving full autonomous flight capabilities on a Rotary Wing platform.

The control system architecture used to control the helicopter is based on a nested PID Approach. The Vx and Vy track velocities control is implemented using a two levels, nested loop structure. Lateral track velocity (Vy) errors are used to generate roll demands for the roll (phi) control module, while longitudinal track velocity (Vx) errors are used to generate pitch demands for the pitch (theta) control module. The inner attitude controllers generate commands to maintain the desired helicopter reference conditions.

The reference track velocities Vx and Vy can be generated either by an outer guidance and navigation control system or by a user pre-defined reference velocity profile.

The vertical velocity control uses a stand alone PI feedback control loop, while heading is controlled by a loop closed on the onboard gyroscope control unit

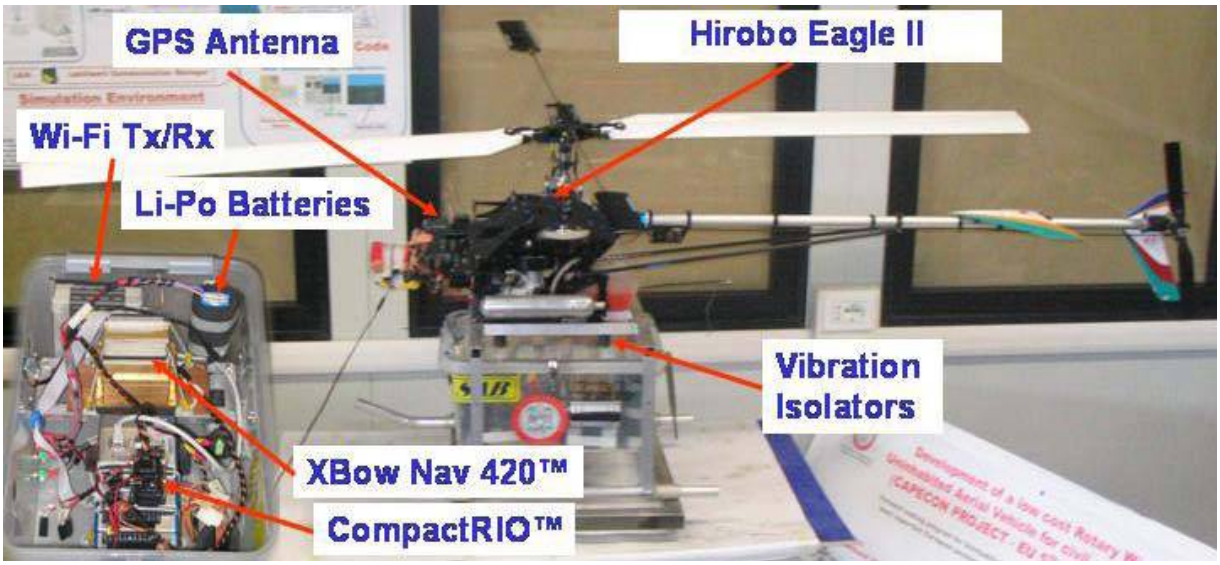


*Figure 1: UNIBO Rotary wing UAV*

Preliminary flight tests showed that it has sufficient controllability and robustness for the maneuvers required for slow hover-like flight. [2, 9]

## 2. ON-AXIS IDENTIFICATION

At the beginning, the helicopter longitudinal and lateral dynamics were considered as totally separated without any off-axis effect.

The adopted Time-domain identification procedure is based on the comparison between the (real) measured signal and the simulated one. Figure 2 shows a schematic representation of the procedure for longitudinal dynamics on-axis identification in Open loop chain.

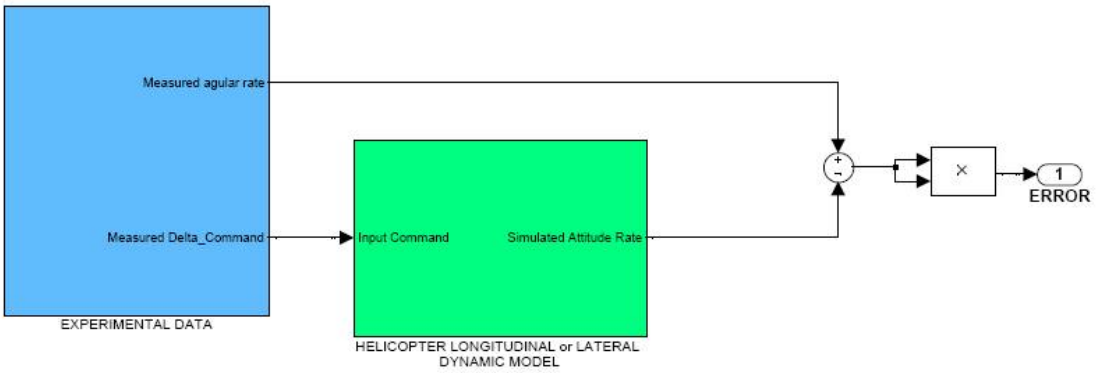


*Figure 2: Open Loop On-axis Identification*

The cost function (1) is the sum of the errors between the measured and simulated signals and is minimized in order to find the optimum transfer function parameters. Sum is performed every computing task, with a simulation step time equal to 0.01 s.

$$CostFunction = \sum (Ymeas - Ysim)^2 \tag{1}$$

Once parameters have been computed by minimizing the cost function over a *training data set*, *cross-validation* is performed using totally new a data set (fresh data, [4]).
Author's scripts have been used in order to find the unknown parameters value by minimizing a *Cost Function* (generally related to the particular identification test) using MATLAB@ function [3]:

***FMINSEARCH:*** *Multidimensional unconstrained nonlinear minimization*

In order to test fitting performances, the following *goodness of fit* index [4] has been computed:

$$R^2 = 1 - \frac{\sum (Ymeas - Ysim)^2}{\sum (Ymeas - mean(Ymeas))^2}$$

where *Ymeas* and *Ysim* are, respectively, the measured and simulated data.
This index relates better agreements to numbers near unity. Since $R^2$ value depends on particular test (*Ymeas*), it is more correct to use it for comparing different models over the same inputs rather than to assess goodness of fit of one single model. Moreover $R^2$ can be also NEGATIVE (typically when the error is, on average, greater then the amplitude of signal) anyway, and also in this case the GREATER is $R^2$ the BETTER is the fitting goodness of the model.

### 2.1 Pitch and roll rate

Following a classical approach [1], second order transfer functions for the pitch and roll rates responses to pilot inputs have been considered (2, 3), and the relative parameters have been identified for several frequency sweeping commands [2].

$$\frac{q}{\delta lon} = \frac{-Alon}{\tau_e} \frac{\omega_{nq}^{\ 2}}{s^2 + 1/\tau_e s + \omega_{nq}^{\ 2}} \tag{2}$$

$$\frac{p}{\delta lat} = \frac{Blat}{\tau_e} \frac{\omega_{np}^{\ 2}}{s^2 + 1/\tau_e s + \omega_{np}^{\ 2}} \tag{3}$$

For longitudinal dynamic the following values were identified:

$$\omega_{nq} = 12.1 \ \ (rad/s) \qquad Alon = 0.2488 \ \ (rad/rad) \qquad \tau_e = 0.132 \ \ (s)$$

while, for lateral dynamic, they have been identified in:

$$\omega_{np} = 18.1 \ \ (rad/s) \qquad Blat = 0.22 \ \ (rad/rad) \qquad \tau_e = 0.132 \ \ (s)$$

More details and initial values computation are reported in [2].
Figure 3 gives evidence of training data and Figure 4 of cross-validation data. In particular left column figures show longitudinal dynamics while right column ones show lateral, response angular rates are in the upper boxes while commands are in the below boxes.

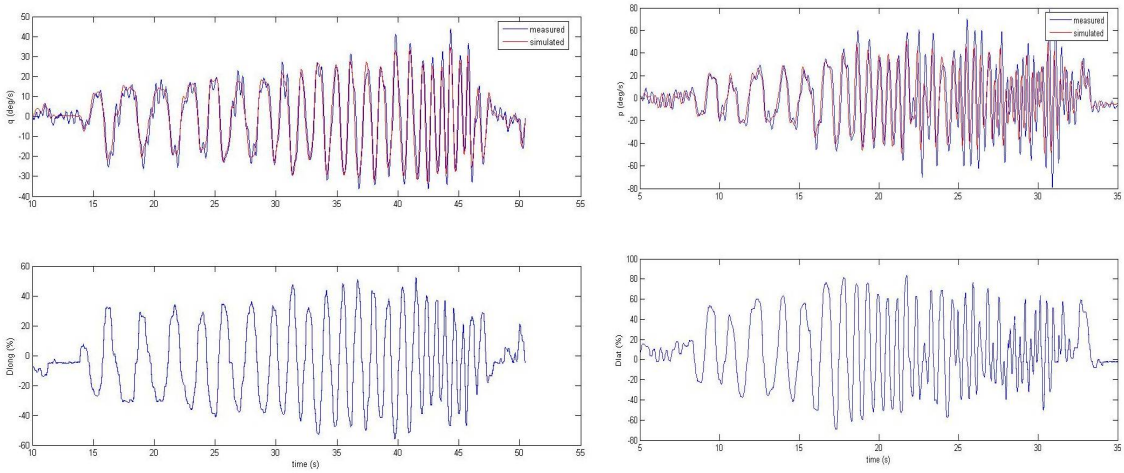


*Figure 3: Longitudinal (left) and Lateral (right) sweeping input commands (below) and relative angular rates (upper) used for system training*

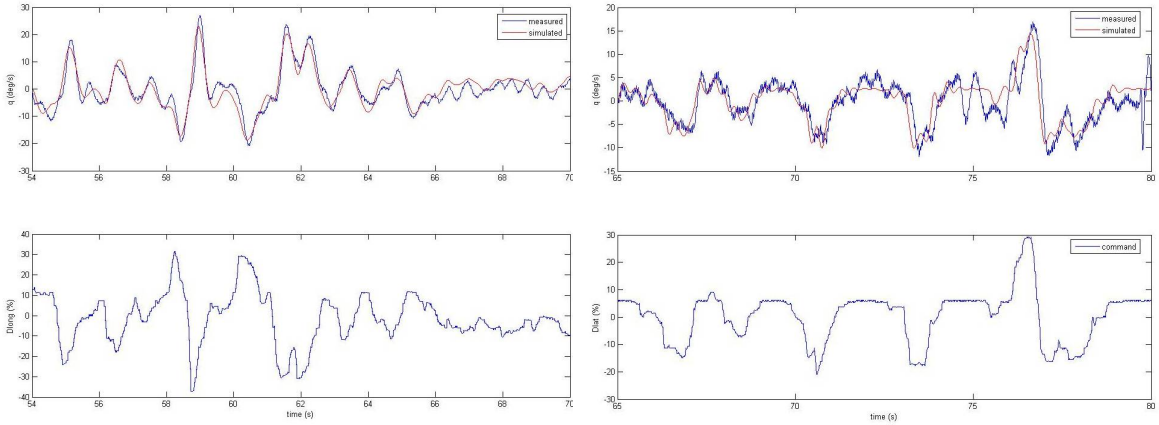


*Figure 4: Longitudinal (left) and Lateral (right) validation input commands (below) and relative angular rates (upper) used for system validation*

For longitudinal cross-validation test goodness of fit index have been computed in $R^2$=0.8586 while for lateral validation $R^2$=0.6085. In this case a better agreement of longitudinal model validation can effectively be seen also 'by eye'.

Then, in body-frame reference, first order attitude-velocity transfer functions (4) have been chosen, and relative parameters have been identified using different usual flight maneuvers (near hovering conditions [5]).

$$\frac{u}{\theta} = \frac{-g}{s - X_u} \qquad \frac{v}{\phi} = \frac{g}{s - Y_v} \tag{4}$$

In both cases *g* parameter was assumed to be equal to 9.81 m/s$^2$ (gravity acceleration) and the remaining parameters have been identified.
Figures 5 and 6 show *training* and *cross-validation data* sets for attitude-velocity transfer functions (left column: longitudinal, right column: lateral, upper fig.; body frame velocity, below figure: input command).

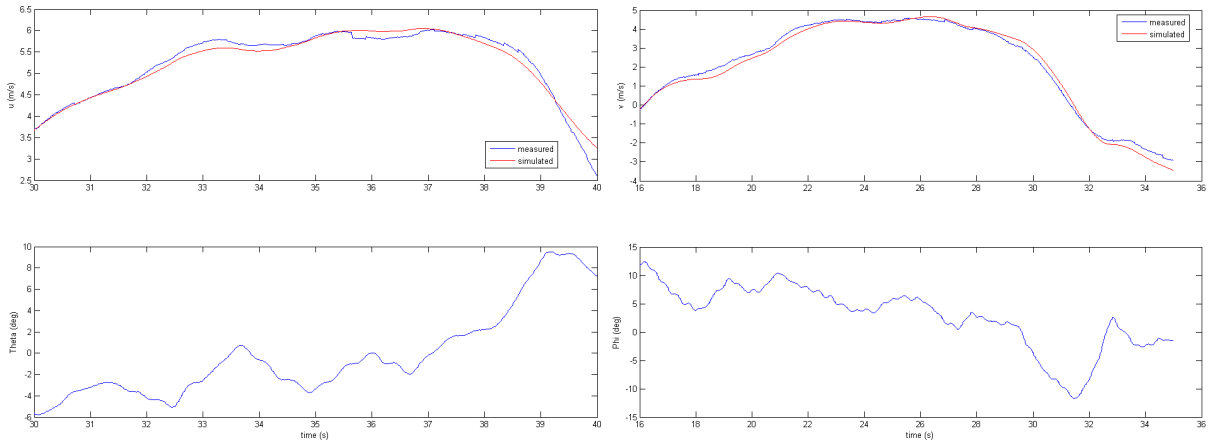


*Figure 5: Input commands (below) and relative speeds (upper) for Longitudinal (left) and Lateral (right) velocity model Identification*

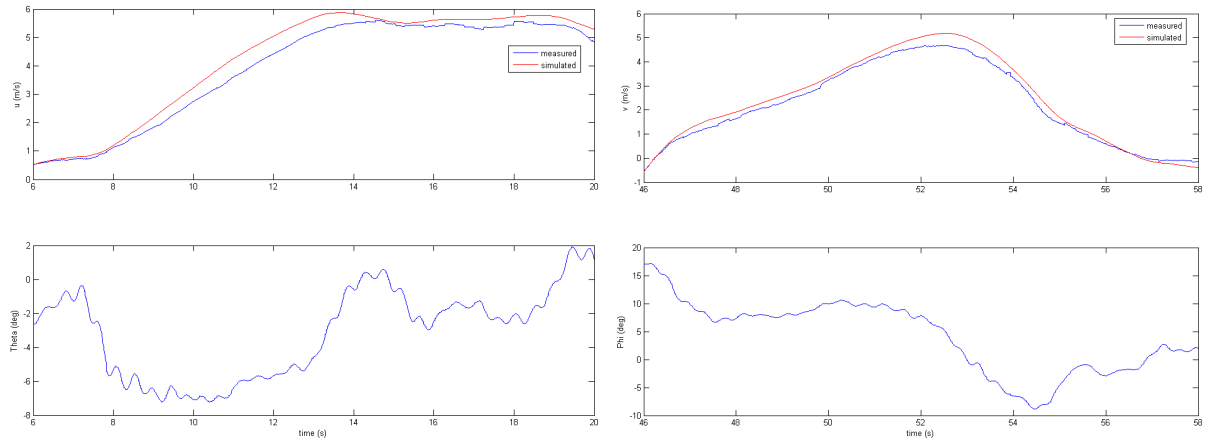


*Figure 6: input commands (below) and relative speeds (upper) for Longitudinal (left) and Lateral (right) velocity model Validation*

Using the cost function defined in (1), the following identified parameters were computed:

$$X_u = -0.052 \ (1/s) \qquad Y_v = -0.046 \ (1/s)$$

with respectively a validation goodness of fit index of $R^2$=0.9366 for longitudinal dynamics and $R^2$=0.9586 for lateral,

## 2.1 Vertical speed dynamic

Vertical dynamics have been modeled using a first order transfer function from command to velocity [1]:

$$\frac{w}{\delta coll} = \frac{Zcoll}{s - Z_w} \tag{5}$$

Figure 7 shows *training* and *cross-validation* data sets used for heave dynamic transfer functions identification.

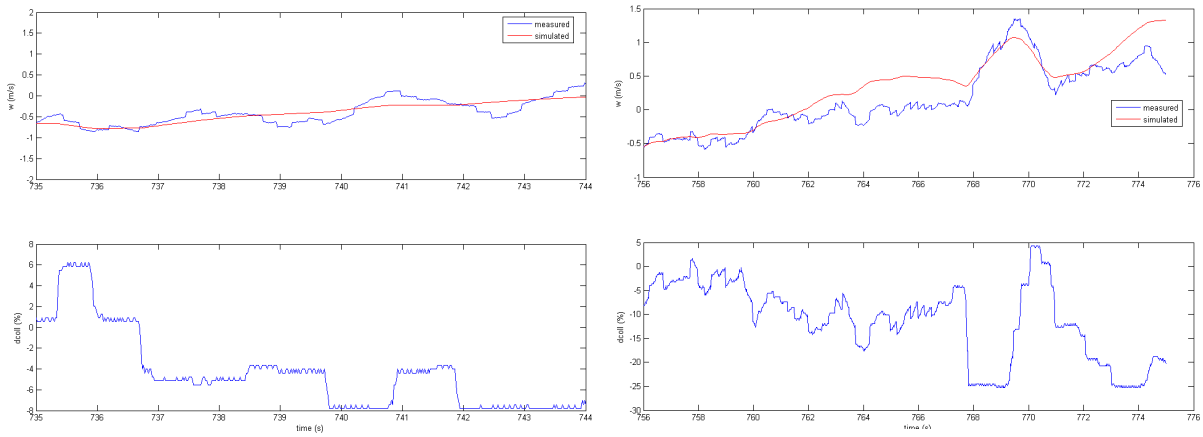


*Figure 7: Training (left) and validation (right) data sets for heave dynamic transfer functions (upper: vertical velocity, below: collective input command)*

The relative derivatives have been identified in:

$$Z_{coll} = -7.7330 \quad (m/(s^2 \cdot rad))$$
$$Z_w = -0.3567 \quad (s^{-1})$$

with a validation test goodness of fit index of $R^2$=0.7127.

Table n.1 summarizes the values found for the On-Axis parameters found using Open Loop identification:

| Name | ***Xu*** | ***Yv*** | ***Alon*** | ***Blat*** | ***tf*** | ***Xa*** | ***Yb*** | ***g*** | ***Lb*** | ***Ma*** | ***Zcoll*** | ***Zw*** |
|---|---|---|---|---|---|---|---|---|---|---|---|---|
| Value | 0.052 1/s | 0.046 1/s | 0.2488 rad/rad | 0.22 rad/rad | 0.132 s | 9.81 m/(s$^2$·rad) | 9.81 m/(s$^2$·rad) | 9.81 m/s$^2$ | 327.6 1/s$^2$ | 146.4 1/s$^2$ | -7.733 m/(s$^2$·rad) | -0.3567 1/s |

*Table 1: On-axis Open Loop Identified Values using a pure longitudinal or lateral maneuver*

## 3. OFF-AXIS IDENTIFICATION IN OPEN LOOP

The below system (6) describes the model used for Off-axis Open Loop identification tests. In this system, equations present both the On-Axis parameters values (just identified as reported in Table1) and new 11 Off-axis derivatives (reported in right column) to be identified

$$
\begin{aligned}
\dot{u} &= X_u \cdot u - g \cdot \theta + X_a \cdot a \\
\dot{v} &= X_v \cdot v + g \cdot \phi + Y_b \cdot b \\
\dot{p} &= L_b \cdot b + L_a \cdot a + L_u \cdot u + L_v \cdot v \\
\dot{q} &= M_a \cdot a + M_b \cdot b + M_u \cdot u + M_v \cdot v + M_{col} \cdot \delta coll \\
\dot{\phi} &= p \\
\dot{\theta} &= q \\
\dot{a} &= -q - \frac{a}{\tau_f} + \frac{A_b}{\tau_f} \cdot b + \frac{A_{lon}}{\tau_f} \cdot \delta lon + \frac{A_{lat}}{\tau_f} \cdot \delta lat \\
\dot{b} &= -p - \frac{b}{\tau_f} + \frac{B_a}{\tau_f} \cdot a + \frac{B_{lat}}{\tau_f} \cdot \delta lat + \frac{B_{lon}}{\tau_f} \cdot \delta lon \\
\dot{w} &= Z_w \cdot w + Z_{Coll} \cdot \delta coll
\end{aligned}
\qquad
\begin{aligned}
&L_a ? \\
&M_b ? \\
&L_u ? \\
&L_v ? \\
&M_u ? \\
&M_v ? \\
&A_b ? \\
&B_a ? \\
&A_{lat} ? \\
&B_{lon} ? \\
&M_{col} ?
\end{aligned}
\qquad (6)
$$

This system can be written in the State Space form:

$$
\begin{aligned}
\dot{x} &= \mathrm{A} \cdot x + \mathrm{B} \cdot u \\
y &= C \cdot x + D \cdot u
\end{aligned}
$$

where the input command vector is: $u = [\delta lon, \delta lat, \delta coll]^T$

the state vector is: $x = [u, v, p, q, \phi, \theta, a, b, w]^T$

the output vector is: $y = [u, v, p, q, \phi, \theta, w]^T$

and:

$$
A = \begin{bmatrix}
Xu & 0 & 0 & 0 & 0 & -g & Xa & 0 & 0 \\
0 & Yv & 0 & 0 & g & 0 & 0 & Yb & 0 \\
Lu & Lv & 0 & 0 & 0 & 0 & La & Lb & 0 \\
Mu & Mv & 0 & 0 & 0 & 0 & Ma & Mb & 0 \\
0 & 0 & 1 & 0 & 0 & 0 & 0 & 0 & 0 \\
0 & 0 & 0 & 1 & 0 & 0 & 0 & 0 & 0 \\
0 & 0 & 0 & -1 & 0 & 0 & -1/\tau_f & Ab/\tau_f & 0 \\
0 & 0 & -1 & 0 & 0 & 0 & Ba/\tau_f & -1/\tau_f & 0 \\
0 & 0 & 0 & 0 & 0 & 0 & 0 & 0 & Zw
\end{bmatrix}
\qquad
B = \begin{bmatrix}
0 & 0 & 0 \\
0 & 0 & 0 \\
0 & 0 & 0 \\
0 & 0 & Mcoll \\
0 & 0 & 0 \\
0 & 0 & 0 \\
Alon/\tau_f & Alat/\tau_f & 0 \\
Blon/\tau_f & Blat/\tau_f & 0 \\
0 & 0 & Zcoll
\end{bmatrix}
$$

$$
C = \begin{bmatrix}
1 & 0 & 0 & 0 & 0 & 0 & 0 & 0 & 0 \\
0 & 1 & 0 & 0 & 0 & 0 & 0 & 0 & 0 \\
0 & 0 & 1 & 0 & 0 & 0 & 0 & 0 & 0 \\
0 & 0 & 0 & 1 & 0 & 0 & 0 & 0 & 0 \\
0 & 0 & 0 & 0 & 1 & 0 & 0 & 0 & 0 \\
0 & 0 & 0 & 0 & 0 & 1 & 0 & 0 & 0 \\
0 & 0 & 0 & 0 & 0 & 0 & 0 & 0 & 1
\end{bmatrix}
\qquad
D = \begin{bmatrix}
0 & 0 & 0 \\
0 & 0 & 0 \\
0 & 0 & 0 \\
0 & 0 & 0 \\
0 & 0 & 0 \\
0 & 0 & 0 \\
0 & 0 & 0
\end{bmatrix}
$$

This system is similar to the one used by Mettler in [6,7], excepted for the absence of pedal input and yaw dynamic: in small scale helicopters, the cross effects due to yaw dynamic are close to zero and therefore often negligible (values equal to zero in [6]).
As in [7], *Mcoll* derivative have been added in B matrix to account also cross-effect of collective input into longitudinal dynamic.

The first 7 parameters *Ab, Ba, Alat, Blon, Ma, Lb, Mcol* have been identified using again several frequency sweeping inputs near hovering condition [1].
After many tests we found that, as suggested by Mettler [8], it can be set *Ab=Ba=0.* Furthermore, since MATLAB@ *fminsearch* function seems to work better with a maximum of 5 parameters, reducing the number of parameters to be identified it is also desirable.

Now, a new cost function, reported in Fig. 8, that takes into account both errors in longitudinal and in lateral attitude was adopted:

$$CostFunction = \sum ((Phi\_meas - Phi\_sim)^2 + (Theta\_meas - Theta\_sim)^2)$$

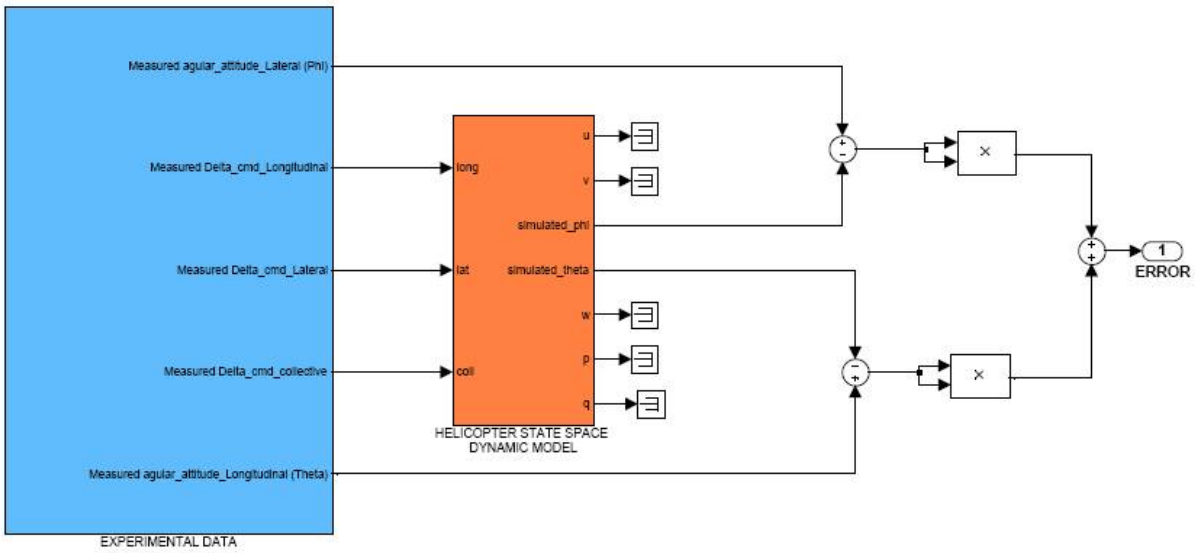


*Figure 8: Off-axis Derivatives Open Loop Identification*

Recorded frequency sweeping input commands have been used in input to the model both for longitudinal and for lateral dynamics and, as expected, a great improvement has been noticed in reducing attitude drifts of the No-Cross-effect-Model (NCM).
Figures 9 and 10 report training experiments with longitudinal (Fig.9) and lateral (Fig.10) excitements; blue signals represent recorded data, while red ones belong to the cross-effect model and green ones to the NCM. The left (pitch angles) and right (roll angles) boxes are, for each figure, relative at the same data set, and we can notice how the cross identification reduce errors in both attitude angles.

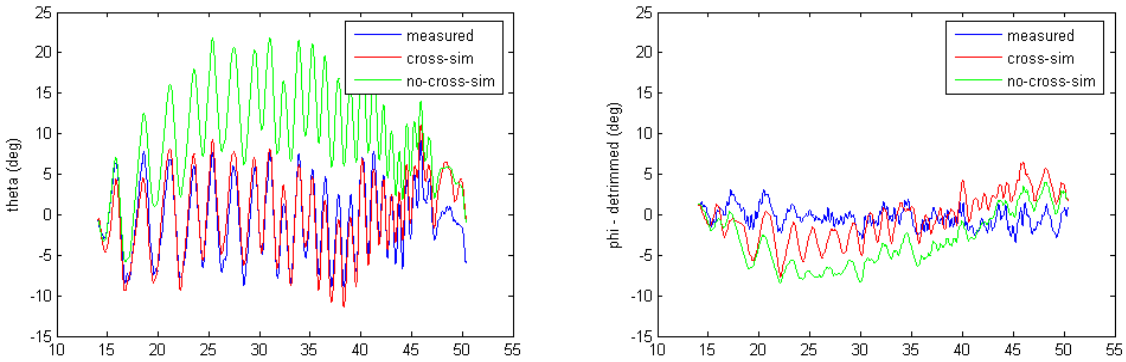


*Figure 9: Off-axis Derivatives Open Loop Identification - Longitudinal training data set (Left: pitch angle, Right: roll angle.)*

Longitudinal test goodness of fit is $R^2$= 0.7353 (vs $R^2$= -5.5632 for NCM) for theta angle and of $R^2$= -1.5551 for phi (vs $R^2$= -12.5321 for NCM): the fit function show a clear increase in attitudes estimation.

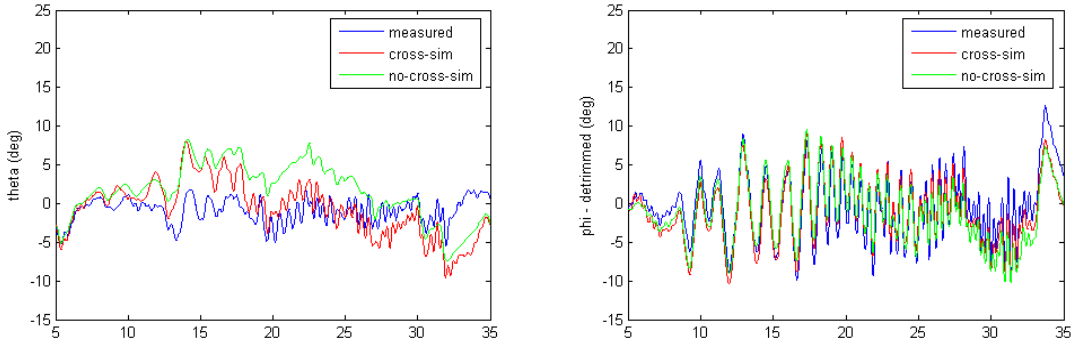


*Figure 10: Off-axis Derivatives Open Loop Identification - Lateral training data set (Left: pitch angle, Right: roll angle.)*

Also for lateral sweeping test a good improvement can be seen in signals fitting, and it can be noticed how certain helicopter responses are now present in the cross-effects model (e.g. Fig. 10, left, red vs green signal for the roll angle, t=20...25s). In this case test goodness of fit is $R^2$=-3,4643 (vs $R^2$=-6.5254 for NCM) for theta angle and $R^2$=0.7616 for phi (vs $R^2$=0.6636 for NCM).

Starting point for derivatives identification procedure was a set of 'zero values'.

In all test cases, in order to verify that a global minimum of the cost function (and not to a local one) was found, all the runs were repeated with different initial conditions.

Analyzing identified values (Table2) it can be seen that the parameters have different values if identified with longitudinal or lateral and, sometimes, they present also a change in sign., As a consequence, it was decided to assume mean values for these parameters obtaining a sort of 'mean system' and to measure goodness of fit of this new model with cross-validation tests only.

| **Derivative** | Longitudinal Test Value | Lateral Test Value | **OL Mean value** |
|---|---|---|---|
| ***Alat*** *(-)* | 0.2023 | -0.0446 | **0.0789** |
| ***Blon*** *(-)* | 0.0655 | -0.0648 | **3.5000e-004** |
| ***La*** *(-)* | -0.5404 | 173.4853 | **86.4724** |
| ***Mb*** *(-)* | -37.4823 | -69.9203 | **-53.7013** |
| ***Mcoll*** *(1/s$^2$)* | -21.8085 | -12.3811 | **-17.0949** |
| ***Mu,Mv,Lu, Lv*** *(rad/(m s))* | Set to 0 | Set to 0 | Set to 0 |

*Table 2: Off-axis Open Loop Identified Values using a pure longitudinal or lateral maneuver*

Using *mean values* for *Alat, Blon, Ma, Lb* and *Mcoll* derivatives makes the model to assume a *mean behavior* between the one optimized with longitudinal values only and the one with lateral values. This behavior has been noticed in every validation test performed.

Figure 11 shows the cross-validation of the final system with longitudinal and lateral flight real data.

Longitudinal cross-validation test goodness of fit is $R^2$=0.7549 (vs $R^2$= -0.2332 for NCM) for theta angle and $R^2$= -0.7291 for phi (vs $R^2$= -0.7301 for NCM).

Lateral Cross-validation test, instead, shows goodness of fit of $R^2$= -0.3219 (vs $R^2$= -2.0041 for NCM) for theta angle and of $R^2$= 0.1903 for phi (vs $R^2$= 0.1058 for NCM).
Again, cross-effect model shows a better agreement than NCM especially in longitudinal dynamics, and it can be seen (Fig 11, right column, phi signal e.g. t=74s) that the final model captures some off-axis dynamics.

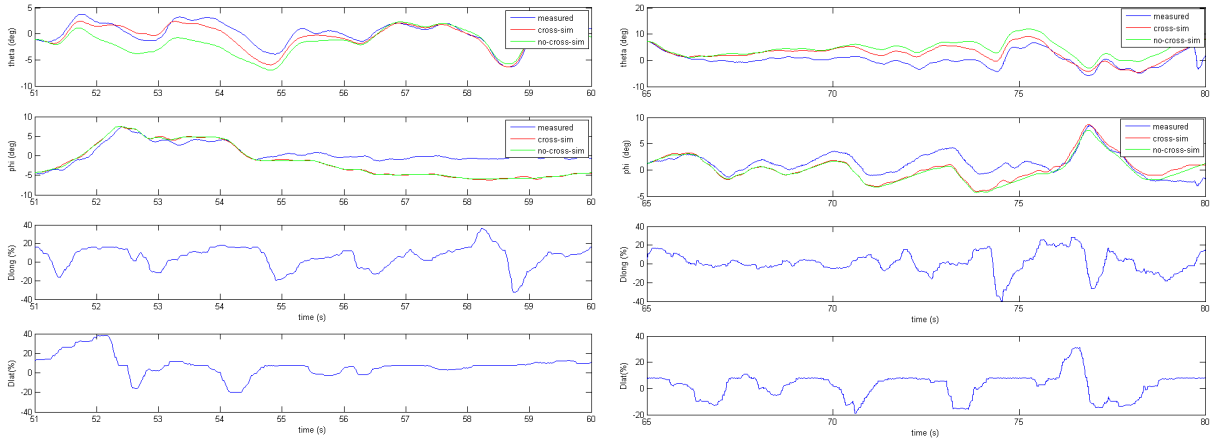


*Figure 11: Open Loop Validation - Longitudinal (left column) and Lateral maneuvers (right column),*

The OL identification procedure for speed derivatives *Mu*, *Mv*, *Lu*, *Lv*, was done using zero as starting values for the optimization algorithm, since the flying tests used were relative to flights near hovering conditions.
However, probably due to too big drifts in simulated speed signals, it was not possible to find a set of values different from zero providing a better agreement in cross-validation tests.
Therefore, zero values for *Mu*, *Mu*, *Lu*, *Lv*, have been used as starting point for CL identification tests (see section 4).

## 4. OFF-AXIS IDENTIFICATION IN CLOSED LOOP

During closed loop identification the already mentioned 9 parameters *Alat*, *Blon*, *La*, *Mb*, *Mu*, *Mv*, *Lu*, *Lv*, *Mcol were initialized using*, the OL identification mean values.

The adopted closed loop identification procedure is based on the control architecture, shown in Figure 12. In this procedure, real measured set-point values and the relative off-axis commands are the model inputs (e.g. *U_set_point+dlat+dcoll* for longitudinal, *V_set_point+dlong+dcoll* for lateral maneuvers), while the attitude error (difference between real and predicted output of the outer control loop) and the command error (difference between real and predicted output of the inner control loop) are used to compute the new cost function. For example in longitudinal maneuvers:

$$CostFunction = \sum ((Theta\_meas - Theta\_sim)^2 + (dlong\_meas - dlong\_sim)^2)$$

while in lateral maneuvers:

$$CostFunction = \sum ((Phi\_meas - Phi\_sim)^2 + (dlat\_meas - dlat\_sim)^2)$$

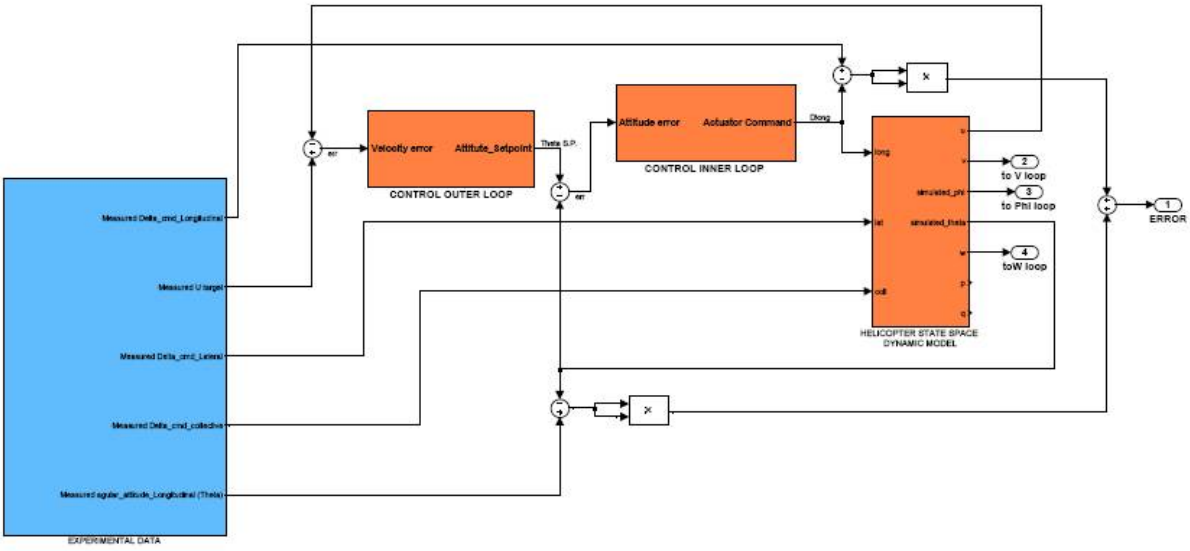


*Figure 12: Closed Loop Identification logic*

The following table reports the identified values during step-like cross-validation velocity maneuvers.

| Derivatives | OL (Mean) | CL longitudinal | CL lateral | CL Mean |
|---|---|---|---|---|
| **Alat** *(-)* | 0.0789 | 0.1328 | 0.0777 | **0.1053** |
| **Blon** *(-)* | 3.5000e-004 | 2.9896e-004 | 3.4119e-004 | **3.2008e-004** |
| **La** *(-)* | 86.4724 | 157.4712 | 89.2649 | **123.3681** |
| **Mb** *(-)* | -53.7013 | -108.0648 | -55.6379 | **-81.8513** |
| **Mu** *(rad/(m s))* | 0 | -0.0053 | 6.4525e-005 | **-0.0026** |
| **Mv** *(rad/(m s))* | 0 | -0.0018 | -1.6989e-005 | **-9.0849e-004** |
| **Lu** *(rad/(m s))* | 0 | -8.9655e-004 | 1.2198e-004 | **3.8729e-004** |
| **Lv** *(rad/(m s))* | 0 | -0.0026 | -8.7996e-006 | **-0.0013** |
| **Mcol** *(rad/(m s))* | -17.0949 | -17.0854 | -17.1030 | **-17.0942** |

*Table 3: Values Identified in Off-axis Closed Loop (CL)*

Note that, final values are similar to those reported in [6] and [7] for the X-cell, except for La and Mb that are greater than expected but correctly smaller than the on-axis corresponding derivatives Lb, Ma (see Table 1).

About speed derivatives *Mu, Mv, Lu, Lv* , it can be seen how the final values are much smaller than those found in literature for similar rotorcrafts; this, anyway in our opinion, confirms that influence of speed in near hover condition is irrelevant. In fact, Mu=-0.0026 means that a speed of u=2 m/s induces a really poor contribution (0.0052 rad/s$^2$) to pitch acceleration with respect to the contribution of *Ma (e.g. 2.54 rad/s$^2$ with a=1 deg.). Mv* and *Lu* (the off-axis speed derivatives) are even smaller and therefore negligible.

Validation tests of the identified parameters in different closed loop controls are shown both for longitudinal (Fig.13, left column) and lateral (Fig.13, right column) inputs.

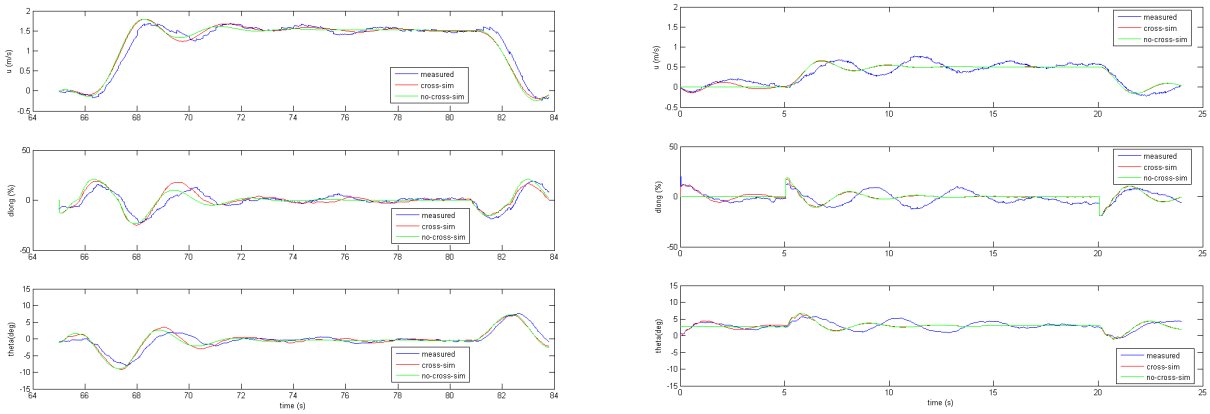


*Figure 13: Closed Loop Validation Tests (upper: velocity, middle: command, below: attitude angle) (left column: longitudinal CL flight, right column: CL lateral flight)*

| GIF index | Longitudinal | Longitudinal NCM | GIF index | Lateral | Lateral NCM |
|---|---|---|---|---|---|
| $R^2$ *u* | 0.9525 | 0.9447 | $R^2$ *v* | 0.8080 | 0.7861 |
| $R^2$ *theta* | 0.7886 | 0.7699 | $R^2$ *phi* | 0.3153 | 0.2206 |
| $R^2$ *dlong,* | 0.6449 | 0.6229 | $R^2$ *dlat* | 0.1973 | 0.0598 |

*Table 4: Closed loop Goodness of Fit Indexes comparison*

Finally, table 4 gives final evidence that accounting of cross-effects in dynamic model brings to a better agreement of the model regarding speeds, attitude angles and closed loop commands and that this improvement exists both for longitudinal and lateral dynamics.

## 5. CONCLUSIONS AND OUTLOOK

A simple identification procedure, developed in a Matlab-Simulink environment, in order to obtain a representative dynamic model of a small rotorcraft UAV near hovering flight condition has been presented. Open-loop identification sessions both with and without cross-effects have been shown; a parameters refinement through a particular closed loop identification technique was then performed. For each test, indexes of relative goodness of fit have been presented demonstrating the benefits of the new model.

The identified model will be used for control design purposes, so it will be possible, using MATLAB@ *signal constraint blockset,* to pre-tune controller gains, giving a set of control target performances as *raise time, maximum overshoot* and *final error.*

Moreover, the authors will identify rotorcraft dynamics also in high speed conditions. The complete derived models (low and high speed) will be used for pre-tuning control helicopter autopilot parameters and to perform comparison between advanced control architecture, based on feed-forward actions, with common control architecture.

## 6. ACNOWLEDGMENT

Authors would like to thank Matteo Zanzi (DEIS, Bologna University) for the needful tips he gave us regarding automatic controls and identification and Veronica Rossi (DIEM, Bologna University) for her constant support during flight tests.

## REFERENCES


[1] B.Mettler **"***Identification Modeling and Characteristics of Miniature Rotorcraft*", Kluwer Academic Publishers, Boston M.A., USA, 2003

[2] R.Pretolani, G.M.Saggiani, V.Rossi, B.Teodorani *"An "off the shelf" avionics system for Rotary Wing UAV rapid prototyping*"**,** Proceedings of the 32nd European Rotorcraft Forum, Maastrich (The Netherlands), Sept. 2006, paper ID UA03

[3] MATLAB@ help guide

[4] L.Ljung: **"***System Identification - Theory For the User"*, PTR Prentice Hall, Upper Saddle River, N.J., 1999

[5] C.Castillo, W.Alvis, M.Castillo-Effen, K.VAlavanis, W.Moreno, *"Small scale helicopter analysis and controller design for non-aggressive flights"*, Proceedings of IEEE SMC Conference, Hawaii, 2005

[6] B.Mettler, M.Tischler, T.Kanade "*System identification of a small-sized unmanned Helicopter Dynamics*"**,** American helicopter society 55° annual forum, 1999

[7] B.Mettler, M.Tischler, T.Kanade, *"System identification modeling of a small-scaled unmanned Rotorcraft for flight control design"*, Journal of American Helicopter Society, 2001

[8] B.Mettler, C.Dever, E.Feron, *"Scaling effects and dynamic Characteristics of Miniature Rotorcraft"*, *AIAA*, Journal of Guidance, Control, and Dynamics, Vol.27, No.3, 2004

[9] R.Pretolani, G.M.Saggiani, V.Rossi, B.Teodorani, F.Zanetti, '*Sviluppo di un sistema ad ala rotante con avionica"COTS"*, XIX AIDAA National Congress, September the 17-21, 2007 Forlì (FC)